Oxidation of CO on a Pt−Fe Alloy Electrode Studied by Surface Enhanced Infrared Reflection−Absorption Spectroscopy

Masahiro Watanabe,* Yimin Zhu,† and Hiroyuki Uchida

Laboratory of Electrochemical Energy Conversion, Faculty of Engineering, Yamanashi University, Takeda 4-3, Kofu 400-8511, Japan

Received: August 24, 1999

To clarify the CO-tolerant mechanism at Pt-based alloy anode catalysts, surface-enhanced infrared reflection−absorption spectroscopy with the attenuated total reflection technique (ATR-SEIRAS), coupled with CV measurement, was used to observe the oxidation process of adsorbed CO on a typical Pt−Fe (Pt−Fe = 0.27/0.73) alloy. The alloy electrode exhibits a lower saturated coverage of CO ($\theta_{CO} = 0.55$) than that of pure Pt ($\theta_{CO} = 1.0$). The dominating linear CO is observed around 2000 cm^{-1} when the equilibrium adlayer of CO covers the alloy electrode; however, linear and bridged CO and also COOH were found at the pure Pt electrode at the same CO coverage in the non-steady-state. On the basis of our previous results that a Pt skin is formed during the repetitive potential cycling due to the dissolution of Fe on the alloy surface and the skin exhibits less electronic density in the d band, it can be explained that the lowered linear CO coverage and almost no bridged CO are obtained as the result of the lowered back-donation of d electrons from the Pt skin to adsorbates on the alloy surface. The wavenumber shift of the linear CO stretching to a lower value at the alloy, which is not simply predicted by the lowering of the back-donation of the d electron, is ascribed to the weakening of the C−Pt bond. As a presumable effect of the electronic structure change at the Pt skin, the dissociation−oxidation of adsorbed water as well as a formation of adsorbed HOOH species are clearly observed beyond 0.6 V in the electrolyte solution without CO, which is different from that at the pure Pt electrode. Carbonate species can also be detected around 1300−1450 cm^{-1}, which are possibly produced by the surface reaction of CO_2 with water.

Introduction

Electrooxidation of CO and/or poisoning by CO on Pt alloys have been extensively investigated[1−6] in view of the fundamental and practical importance as fuel cell reactions. Designing new catalysts for fuel cells requires an understanding of the chemisorption and the electrocatalytic oxidation of CO, in particular, in the fuels such as gaseous hydrogen derived from steam-reformed hydrocarbons, in which CO is found as a serious impurity. Many experimental results accumulated in our laboratory for various electrocatalysts for fuel cells indicate that the alloying of Pt with the other transition metals enhances significantly the electrocatalytic activities of Pt, e.g., for the CO-tolerant H_2 oxidation or the O_2 reduction.[7−11] We have also shown that the hydrogen oxidation at pure Pt electrocatalysts is completely poisoned in the presence of only 10 ppm of CO,[12] while a content of CO in re-formates prepared by conventional procedures is about 1% in general. Studies on the CO oxidation at these electrocatalysts are helpful to understand not only the poisoning mechanism but also the surface characteristics of the electrocatalysts. In our laboratory, Pt−Fe alloys have been found to be excellent CO-tolerant anode catalysts as well as Pt−Ru, Pt−Co, Pt−Ni, or Pt−Mo.[10−11] X-ray photoelectron spectroscopy (XPS) analyses of the surfaces after the reactions indicated that the active surfaces were covered with a few monolayers of Pt, because of the dissolution of nonprecious metals from the alloy surfaces. However, photoelectron peaks for the Pt skin positive-shifted from that of pure Pt. This strongly suggests that the density of valence electrons (5d) of the Pt skin on the alloys is lower than that of pure Pt.[7−11] To understand the trends fully, it is necessary to have the detailed quantum-mechanical information about the bonding mechanism between the Pt skin and the bulk alloy. Such information is not available at present. However, the lower electronic density of the d-band in the Pt skin can be easily understood in terms of the orbital mixing. Hybridization of the occupied states of an electron-rich metal (Pt) with the unoccupied levels of an electron-poor metal (Fe or bulk alloy) leads to a loss of Pt character in the occupied states and hence the reduction in the electron density on the Pt skin. On the basis of the results, we have proposed a mechanism for the CO tolerance, i.e., the lowered electron density of the 5d orbital of Pt decreases an electron back-donation from the Pt 5d orbital to the $2\pi^*$ orbital of CO, and consequently suppresses CO−Pt bonding, resulting in the lowered CO coverage.[10,11,13]

Generally, metal surfaces are characterized by using vacuum techniques such as an XPS, a low-energy electron diffraction (LEED), an electron energy lose spectroscopy (EELS), and so on.[14−18] Any conclusion about the mechanism led by these means, however, will require comparison with the results from other experimental techniques. For the practically electrochemical interfaces such as a present case, an in situ spectroelectrochemical characterization is more important, as it can provide a direct information on the interface.

Vibrational spectroscopic techniques can provide information about the mechanism of the electrochemical oxidation of CO

* To whom correspondence should be addressed. Phone: +81-55-220-8620. Fax: +81-55-254-0371. E-mail: mwatanab@ab11.yamanashi.ac.jp.
† On leave from China.

10.1021/jp993001q CCC: $19.00
Published on Web 02/04/2000

adlayer on electrodes. However, to our knowledge, in situ FTIR studies on the oxidation of CO have scarcely been reported for Pt alloy electrodes, except a Pt−Ru alloy and a Pt−Sn alloy.[4,5,19−21] There is no work using the ATR-SEIRAS technique for the Pt−Fe alloy electrode. Most of the studies on the electrooxidation of the CO adlayer using IR spectroscopy involved an external reflection setup, in which the light beam has to pass through at least 10^3 layers of electrolytes before striking the studying surface. Very recently, Osawa and coworkers reported a series of IR spectra obtained on an evaporated gold electrode surface in aqueous electrolyte solution, utilizing surface-enhanced IR reflection−absorption spectroscopy with the attenuated total reflection technique (ATR-SEIRAS).[22−25] Using the ATR-SEIRAS technique, we have successfully observed the electrooxidation of the CO adlayer incorporating with adsorbed water at a pure Pt electrode.[26] In this work, we report the ATR-SEIRAS results on the potential-dependent adsorption and oxidation of CO at the Pt−Fe alloy electrode on a silicon prism surface in 0.1 M perchloric acid in comparison with those at a pure Pt electrode. We will also report the dissociation behavior of the adsorbed water molecule. All these results support the mechanism for the CO tolerance at the H_2 oxidation on Pt-based alloys strongly, which recently we proposed.[10,11,13]

Experimental Section

The configuration of the spectroelectrochemical cell used in the present work was similar to that described in refs 22 and 26. The working electrode was a thin Pt−Fe alloy film sputtered on a flat plane of silicon hemicylindrical prism (1 cm in radius and 2.5 cm long) by Ar-sputtering pure Pt and Fe targets simultaneously at room temperature with a ULVAC sputtering apparatus (SH33D). The resulting alloy composition was $Pt_{27}Fe_{73}$ determined by gravimetry and fluorescent X-ray analysis (EDX, Horiba XGT-2000V). A crystallographic structure of the alloy was examined with a grazing angle XRD ($\theta = 1°$, MAC Science). The alloy-coated prism was attached to the spectroelectrochemical cell by sandwiching an O-ring. A copper foil, which inserted outside the O-ring and between the cell body and the edge of the alloy film, was utilized to make a connection between the electrode and a potentiostat (EG&G Princeton Applied Research, model 263). Pt gauze and a reversible hydrogen electrode (RHE) were used as the counter and reference electrodes, respectively. All the potentials in this paper are quoted against RHE.

The thickness of the alloy film was measured with an ultramicrobalance (with a precision of 0.1 μg), which resulted in a thickness of about 7 nm. Before the collection of spectroelectrochemical data, fast potential sweeps (500 mV/s) between 0.05 and 1 V were applied to the electrode for the surface cleaning and to obtain the cyclic voltammogram (CV) for the evaluation of the active electrochemical surface areas of the electrode. The surface area was determined by integrating the charge in the region of hydrogen adsorption/desorption in the CV, which was typically about 3 times larger than the geometrical area. Despite the very thin thickness, the electrode showed a good enough electronic conductivity.

Infrared spectra were taken with a Bio-Rad FTS-6000 spectrometer. Unpolarized infrared radiation from a Globar source was focused at the electrode/electrolyte interface by passing through the silicon prism. The incident angle was 70° from the surface normal. The radiation totally reflected at the interface was detected with a liquid nitrogen cooled linearized narrow-band HgCdTe detector (Bio-Rad). The spectral resolution was 8 cm^{-1}.

Water was purified by Nanopure (Barnsted) and distilled with an addition of a small amount of $KMnO_4$ and NaOH. Reagent grade $HClO_4$ (Kanto Chemical Co.) was dissolved in the resulting pure water to obtain 1 M $HClO_4$. The solution was then pre-electrolyzed according to ref 27, followed by further dilution with the purified water to form a 0.1 M $HClO_4$ solution. The electrolyte solution used was the 0.1 M $HClO_4$ solution saturated with high-purity nitrogen. H_2 gas containing CO of 97.9 ppm was used to purge into the electrolyte solution at 0.05 V for 90 min in order to obtain an equilibrium adsorption of CO. Then, CO in the bulk solution was removed by purging with N_2 while keeping the potential constant for 1 h.

Results and Discussion

1. Structural and Electronic Properties of $Pt_{27}Fe_{73}$ Alloy. X-ray diffractions of the alloy indicated the formation of a solid solution phase with a face-centered cubic (fcc) crystal structure, where the preferential exposure of (111) facets and additionally (200), (220), (311), and (222) similar to those of pure Pt were seen.

To obtain a steady electrode surface condition, the repetitive cycling of potentials is performed between 0.05 and 1.0 V. It has been found in our laboratory that the Pt skin forms during the pretreatment due to dissolution of Fe on the surface of Pt−Fe alloys as well as the other Pt alloys with nonprecious metals, which was confirmed by the following facts found by XPS measurement.[7−11,13] A $2p_{3/2}$ peak for the Fe atom could not be observed after the electrochemical pretreatment but those of $4d_{3/2}$ and $4d_{5/2}$ for Pt atom were clearly observed. Generally, the XPS technique can detect elements existing only in a few monolayers on the sample surface. Consequently, the loss of the $2p_{3/2}$ signal for the Fe atom on the surface indicates that the thickness of the Pt skin must be in a few monolayers of the alloy surface. Regardless of the disappearance of Fe atoms at the alloy surface, the binding energies of 4d or 4f of the Pt skin are higher than those of pure bulk Pt, e.g., by about 0.65 and 0.75 eV for $4d_{3/2}$ and $4d_{5/2}$ at the present alloy composition, respectively. These positive chemical shifts corresponding to the less electronic population in the 4d or 4f orbital strongly indicate the increased 5d vacancy or the lower Fermi level of the Pt skin on the alloy. Since the back-donation of 5d electrons has been reported to play a dominant role for the CO chemisorption on bulk Pt,[28] it was reasonable to propose previously by us that the change in the electronic properties of the surface by the presence of the underlying alloy leads to a lower saturated coverage of CO than that of pure Pt, resulting in the higher CO tolerance H_2 oxidation rate. By the present IR measurement, we can expect to obtain new information on the CO adlayer on the skin of the alloy, which may support the above CO tolerance mechanism.

2. Cyclic Voltammometry of the CO Adlayer at a Pt−Fe Alloy Electrode in Perchloric Acid Electrolyte Solution. Figure 1A shows a cyclic voltammogram (CV) on the Pt skin of the Pt−Fe alloy electrode with and without the saturated CO adlayer. Figure 1B shows the CV on the pure Pt electrode with and without the nonsaturated CO adlayer but with the same level of coverage as the Pt−Fe alloy. The coverage of the CO adlayer at the electrodes was evaluated on the basis of the electric charges at the hydrogen adsorption−desorption region. The coverage of the CO adlayer (θ_{CO}) for the Pt skin on the alloy was ca. 0.55, which is much lower than that of about 1.0 at the pure Pt electrode.[26] The θ_{CO} for the pure Pt shown in Figure 1B was ca. 0.50 in a nonsaturated coverage.

In comparison with the blank CV on the pure Pt (solid line), it is clear that the blank anodic current on the Pt skin of the

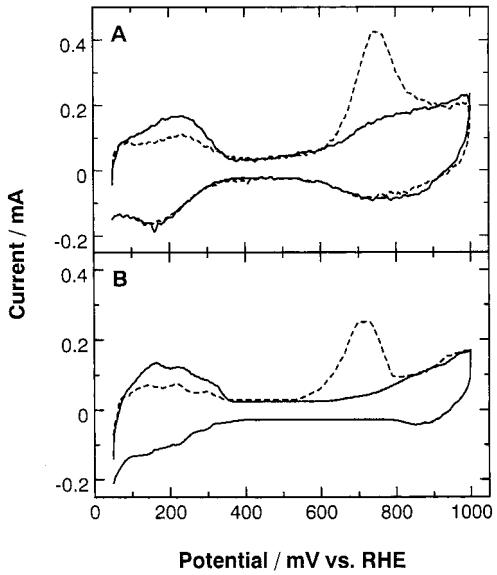

Figure 1. Cyclic voltammograms (20 mV/s) on a sputtered $Pt_{27}Fe_{73}$ alloy film electrode (A) and on a pure Pt electrode (B) with (dashed line) and without (solid line) a CO adlayer of ca. 0.5 coverage in 0.1 M $HClO_4$.

alloy electrode (solid line) commences to increase at about 0.6 V, which is ca. 0.2 V less positive than that of the former and shows a larger current at more positive potentials. The total charges for the anodic and cathodic currents, which correspond to the adsorption−desorption of the OH species produced by the oxidation of adsorbed water molecules and by the reduction of the OH species, are also larger than those of the pure Pt. This result indicates that the Pt skin surface on the alloy has a larger affinity or an oxidative property to water molecules than the bulk pure Pt. On the alloy electrode with the saturated CO adlayer, the anodic current for the CO oxidation begins to increase at about 0.6 V, corresponding to the onset of the water molecule oxidation or the adsorption of OH species, and shows only one anodic peak at 0.73 V without any preshoulder or shoulder peak (see Figure 1A). On the other hand, as shown in Figure 1B, the oxidation of the adsorbed CO on the pure Pt starts at the potential less positive than 0.55 V and shows a peak at ca. 0.7 V via a small preshoulder. The shoulder oxidation current and the less positive onset potential can be ascribed to carboxyl radicals formed on the pure Pt surface.[26] Despite almost the same CO adlayer coverage on the Pt skin and the pure Pt in this case, the electric charge for the CO adlayer oxidation on the former is larger than that of the latter, which indicates that the former adlayer involves CO species with a larger value of electrons per Pt site, associated with the oxidation reaction, not like a carboxyl radical or multifold CO but linear CO.

3. In Situ IR Spectra of the Interfacial Water at the Pt−Fe Alloy Electrode. Figure 2 shows a series of IR reflectance spectra for (A) the Pt−Fe alloy electrode and (B) the pure Pt electrode in 0.1 M $HClO_4$ solution, which is simultaneously recorded with the linear potential sweep from 0.05 to 1.00 V at a rate of 20 mV/s (corresponding to the solid line in Figure 1). Each spectrum was obtained by integrating 14 interferograms to improve the signal-to-noise radio of the spectrum. The acquisition time was about 2.5 s per spectrum. Therefore, the potentials shown in the figure are the averages of every 50 mV interval. The first single-beam spectrum at 0.075 V is chosen as the reference spectrum. The negative-going band near 3350 cm^{-1} is observed on the Pt skin of the alloy at potentials less positive than 0.6 V, which is assigned to the OH stretching of

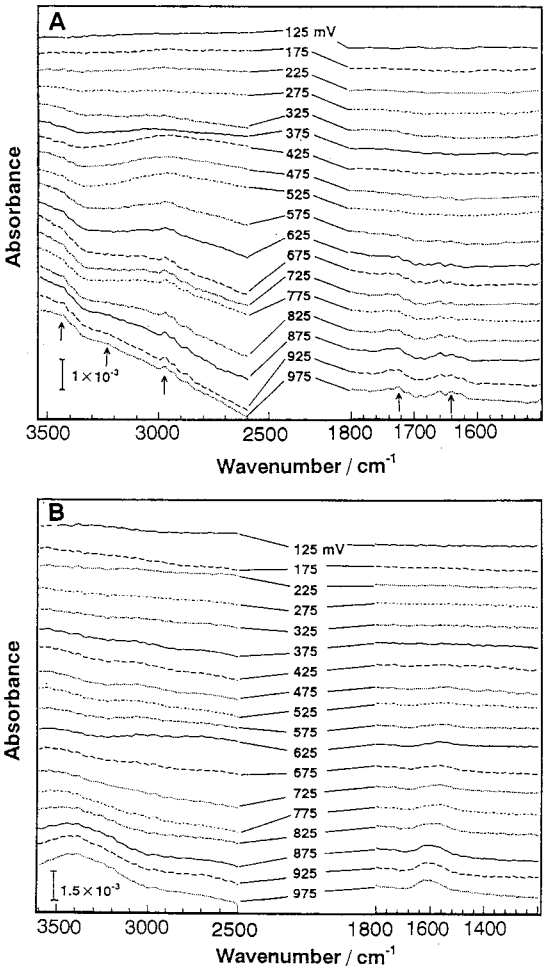

Figure 2. In situ IR spectra taken in 0.1 M $HClO_4$ on the $Pt_{27}Fe_{73}$ film electrode (A) and on the Pt film electrode (B) during a slow anodic scan (20 mV/s). The reference spectrum was the first single-beam spectrum at 0.075 V during the potential sweep.

the adsorbed water.[22−25] The band shifts with increasing potential from a higher to a lower wavenumber, corresponding to a weakening of the OH bond. The negative sign of the band indicates the reduction of the adsorbed water due to its consumption to form some O species. H−O−H bending bands of the adsorbed water molecule are too weak to observe in the region between 1600 and 1800 cm^{-1} below 0.6 V.

Beyond about 0.6 V, however, some new positive-going bands around 3450, 3250, 2960, 1720, and 1640 cm^{-1} can be observed on the Pt skin of the alloy. They may not be assigned to the adsorbed water, since the bands around 3250−2960 and 1720−1640 cm^{-1} are not only too sharp compared with the conventional ones for the adsorbed water, but also split into two sharp bands, and moreover, they are independent of the electrode potential unlike the conventional H_2O. The fact of the simultaneous increase of these band intensities presumably indicates that the bands correspond to a single species, which may be assigned to a peroxide species.[29−31] However, the small sharp band around 2960 cm^{-1} cannot fully exclude the assignment to the CH impurity located between the Si and Pt surfaces, even though the increase in the band intensity with the potential results from its oxidation.

On the pure Pt electrode, the potential-dependent bands near 3400 and 1620 cm^{-1} appear, which can be assigned to the OH stretching and HOH bending vibrations of the adsorbed water. But, no bands near 2960 and 1730 cm^{-1} are observed on the

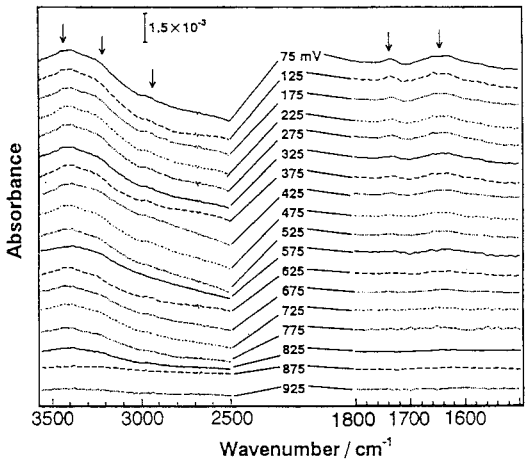

Figure 3. In situ IR spectra taken in 0.1 M $HClO_4$ containing 1.52×10^{-3} M H_2O_2 on the $Pt_{27}Fe_{73}$ alloy film electrode during a slow anodic scan (20 mV/s). The reference spectrum was the last single-beam spectrum at 0.975 V during the potential sweep.

pure Pt electrode. The different adsorption property implies that there is a distinctive difference in the electronic structures between the pure Pt and the Pt skin on the top of the alloy. Obviously, the Pt skin of the Pt−Fe alloy favors the dissociation−oxidation of the adsorbed water beyond 0.6 V. Correspondingly, the anodic current begins to increase at the same potential as seen in Figure 1. The Pt skin with less d electron density may be highly active for the oxidation of the adsorbed water, described by the following sequence of reactions:

$$Pt-OH_2 \rightarrow Pt-OH + H^+ + e^- \quad (1)$$

$$2Pt-OH \rightarrow Pt-O_2H_2-Pt \quad (2)$$

The assignment to the OH or H_2O_2 could be confirmed by the fact that the absorption bands, attributed to HOOH, were seen in the same mid-IR region when H_2O_2 was added into the blank electrolyte solution (its final concentration was 1.52×10^{-3} M), as shown in Figure 3. In this figure, the last single-beam spectrum at 0.975 V was chosen as the reference spectrum since there was more H_2O_2 adsorbed on the surface at the beginning of the positive-going potential sweep, thus the positive bands could be observed. The results demonstrate the infrared vibrations of H_2O_2 to be similar to that observed in Figure 2. The decrease of the band intensities with the potential sweep indicates the further oxidation of H_2O_2.

A metal−molecule interaction may generally lead to an intramolecular bond weakening or dissociation,[7−9] in particular for the oxygen element in the water molecule, by the lateral interaction of the π-orbital of O with empty d_{z^2} orbital of the surface Pt atom or with empty d_{xy} and d_{yz} orbital of dual Pt atoms, respectively. The less 5d electron density of the surface Pt leads to an increased 2π donation to the surface, which strengthens its ability to withdraw electrons from the O atom in the adsorbed water molecule and in turn from the H atom in the adsorbed water. With sweeping potential toward positive, this effect increases. Consequently, the dissociation−oxidation of the adsorbed water molecule becomes easier at the alloy electrode than at the pure Pt electrode. Thus, in situ SEIRAS confirms the perturbation of the electronic structure in the Pt skin by the bulk alloy in the electrochemical environment.

4. In Situ IR Spectra for the Oxidation of the CO Adlayer on the Pt−Fe Alloy Electrode. Infrared reflection spectra for the CO adlayer on the Pt−Fe alloy are shown in Figure 4A,

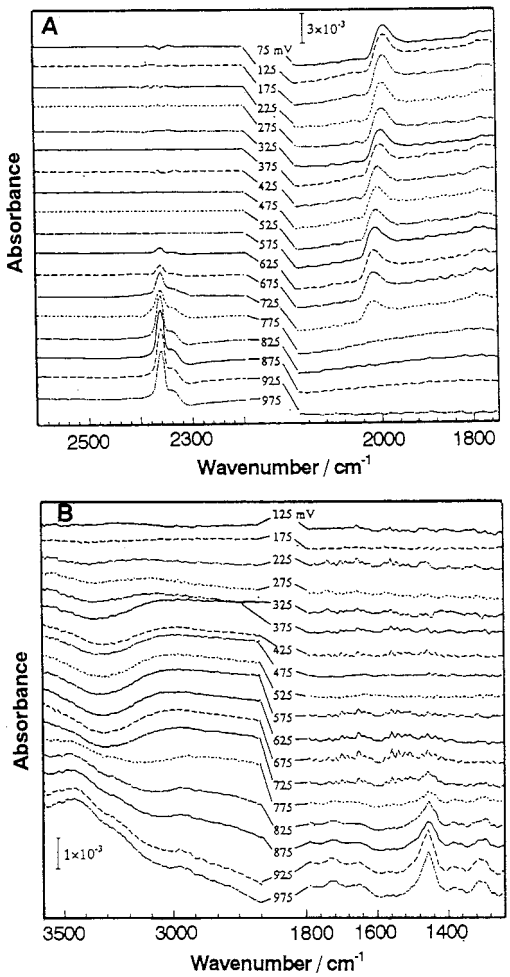

Figure 4. In situ IR spectra taken in 0.1 M $HClO_4$ on the $Pt_{27}Fe_{73}$ film electrode for the saturation coverage of CO ($\theta_{CO} = 0.55$); scan rate 20 mV/s. **(**A) Spectral regions exhibiting the CO and CO_2 absorption bands. The reference spectrum was the single-beam spectrum at about 0.975 V (for no CO) or at about 0.075 V (for no CO_2) during the potential sweep. **(**B) Spectral regions exhibiting the H_2O and OH absorption bands. The reference spectrum was the first single-beam spectrum at 0.075 V during the potential sweep.

which are simultaneously recorded with the linear potential sweep from 0.05 to 1 V. The first single-beam spectrum at 0.075 V (CO_2 free surface) or the last single-beam spectrum at 0.975 V (CO free surface) during potential sweep from 0.05 to 1 V was chosen as the reference spectrum for observing CO_2 or CO, respectively. The absorption bands around 2000 and 2360 cm^{-1} could be assigned to the stretch mode of linearly (atop) bound CO and CO_2, respectively.[26,32,33] The alteration of these absorption bands with the increase of electrode potential indicates the CO oxidation and the CO_2 production. It is obvious that dominating linear CO is observed around 2000 cm^{-1}, which is distinctive from that linear CO (around 2020 cm^{-1}) and bridged CO (around 1850 cm^{-1}) besides COOH coexist at the pure Pt electrode even at the same coverage of CO.[26] The electronic structure of the metal determines which adsorption sites, i.e., on-top, 2-fold, and 3-fold bridges, are occupied for the different metal sites. The presence of the dominating linear CO indicates that there is a smaller back-donation of d electrons at the alloy electrode than that at the pure Pt electrode, which is inferior to the formation of the multifold CO or to the high coverage CO leading to the COOH formation. The result is well consistent with our previously proposed mechanism that the strong

modification in the electronic structure of the Pt skin by the underlying alloy lowers the Fermi level at the electrode surface, which results in deactivation of the Pt skin toward the CO chemisorption, i.e., $\theta_{CO} = 0.55$.

The O−H stretching band near 3400 cm^{-1} of the adsorbed water is observed below ca. 0.75 V (see Figure 4B), which is slightly potential-dependent. The increased negative peak of the absorption band indicates the decrease in the amount of the adsorbed water due to the strong interaction between the water molecule and metal, which also leads to the negative shift of the wavenumber for the stretching. The corresponding O−H bending band between 1600 and 1750 cm^{-1} is too weak to observe below 0.75 V. Whereas the adsorbed HOOH species has been detected at least beyond 0.65 V in the blank solution (see Figure 2), it cannot be detected until the linear CO is almost removed beyond 0.75 V by the oxidation to CO_2. Thus, it is considered that the linear CO on the Pt skin underlain by the Pt−Fe alloy must be oxidized by the reaction with the peroxide species via the so-called "bifunctional mechanism" proposed by Watanabe and Motoo.[1]

$$Pt-OH + Pt-CO \rightarrow 2Pt + CO_2 + H^+ + e^- \qquad (3)$$

Accompanied with the production of CO_2, new bands around 1450, 1380, and 1310 cm^{-1} appear. The bands could be assigned to carbonate species. The carbonate species may be formed through the subsequent steps as in the following

$$Pt-(CO_2) + Pt-OH_2 \rightarrow Pt-CO_3^{2-} + Pt + 2H^+ \qquad (4)$$

where the (CO_2) represents a weakly bonded or nonbonded CO_2 on the Pt skin surface.

Infrared and Raman spectra of carbonates in solutions have been reported by Oliver and Davis.[34] They found that the solvation induced a moderate splitting of the degenerate V3 mode, which led to two peaks at 1376 and 1438 cm^{-1} compared to the 1415 cm^{-1} value for the free carbonate. Iwasita et al. have studied the adsorption of carbonate on Pt(111) and Pt-(110) electrodes.[35] Three bands at 1328, 1455, and 1537 cm^{-1} were likely to be assigned to the adsorbed carbonate species although the authors concluded that the band at 1330 cm^{-1} does not belong to the adsorbed carbonate. In any case, Iwasita et al. concluded that the band near 1455 cm^{-1} is due to vibrations involving the noncoordinated oxygen atoms in the monodentate coordination mode. Very recently, Markovits et al.[36] suggested that the band around 1450 cm^{-1} is more likely due to the bidentate adsorbed carbonate. It has been reported that the symmetric stretching frequency of carbonate complexes is highly sensitive to the environmental conditions (such as an adsorbed water, counterions etc.).[37] Except for the effect of water, the other environmental situation at the interface should be considered. A charge donation to the metal, a vibrational coupling of the adsorbed species, and an electric field of the double layer could alter the band frequency. Generally, the concentration of the carbonate produced from CO_2 should be low in the present acid electrolyte. Therefore, their production must be related to a heterogeneous acid−base reaction, in which the adsorbed water or OH species is involved, as shown by eq 4.

5. Dependence of the Absorption Band for the CO Adlayer on the Electrode Potential. The wavenumber of the linear CO band in the saturated coverage ($\theta_{CO} = 0.55$) on the Pt−Fe alloy electrode is plotted **(▼)** as a functi**o**n of the potential (Figure 5). It was found that the wavenumbers exhibit extremely small values, e.g., ca. 1980 cm^{-1} at 0.05 V, which is 60 cm^{-1} smaller than that of the pure Pt with the saturated coverage CO, i.e., $\theta_{CO} = 1.0$.[26] As the potential is swept more positive between 0.075 and about 0.7 V, the CO band linearly shifts to higher wavenumbers with the slope of about 54 cm^{-1}/V. The slope is larger than that (ca. 30 cm^{-1}/V) of the pure Pt electrode with the saturated coverage of CO, i.e., $\theta_{CO} = 1.0$.[4,26] Generally, the slope increases with the decrease of the coverage. The present large slope is apparently reflecting the suppressed saturating CO coverage on the alloy surface. Two models have been proposed in order to explain such a linear potential dependence on the wavenumber for the CO adlayer, i.e., a first-order "Stark effect" assuming a rigid dipole oscillator in a variable electric field[38] and a "chemical" model of the potential-dependent surface bonding.[39] In addition to the electric field in the inner Helmholz layer, other physical parameters may also influence the wavenumber of the CO adlayer, e.g., the adsorbate coverage and the adsorbate binding geometry. If these physical parameters are constant, the linear frequency−potential relationship can be observed as in the present work on the skin of the Pt−Fe alloy. This linear relationship is quite different not only in the shape but also in the wavenumber location from the nonmonotonic relationship obtained on the pure Pt with the same coverage of CO adlayer, which is shown in Figure 5 by the solid line without individual data points, cited from ref 26. The nonmonotonic relationship on the pure Pt is due to the transition of the bridged CO to the linear CO and maybe due to the effect of the COOH species.[26] The lower d electron density of the Pt skin on the alloy electrode leads to the decrease of the electron back-donation to $2\pi^*$ orbital of the CO, which is one of the dominant factors for the Pt−CO bonding formation,[28] and thus dominating linear CO may be formed, unlike the pure Pt electrode. The decrease of the back-donation might increase the wavenumber for the C−O stretching. In fact, however, the lower C−O wavenumber is observed, as shown in Figure 5. The observed low wavenumber for the C−O stretching indicates that another factor should be considered to understand the experimental fact. For example, the metal−CO molecule interaction must be important. Here, it should also be noted that the half-width (40 cm^{-1}) of the linear CO band on the Pt skin is broader than that (30 cm^{-1}) on the pure Pt.[26] The band broadening mainly reflects the increase in mobility of the adsorbed CO molecules. This implies that the bond length between Pt and C should be increased. The observed low wavenumber of the CO adlayer confirms the increase in the bond length between Pt and C, resulting from the reduction of the Pt−C force constant reflecting the bond length.[40]

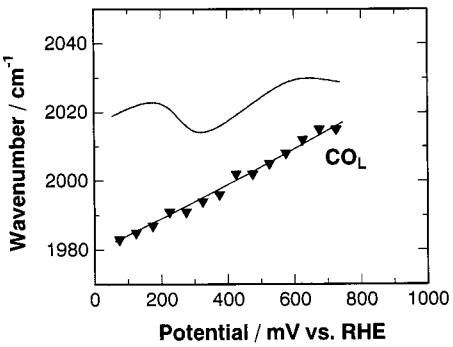

Figure 5. Potential dependence of the stretching vibration wavenumber of the linear CO in the saturated coverage with the CO adlayer of $\theta_{CO} = 0.55$ on the $Pt_{27}Fe_{73}$ film electrode (▼) and of that in approximately the same coverage of nonsaturated CO adlayer on the pure Pt electrode (solid line).

6. CO Tolerance Mechanism on Pt−Fe Alloys for the Oxidation of H_2 Containing CO Impurity. Figure 6 shows

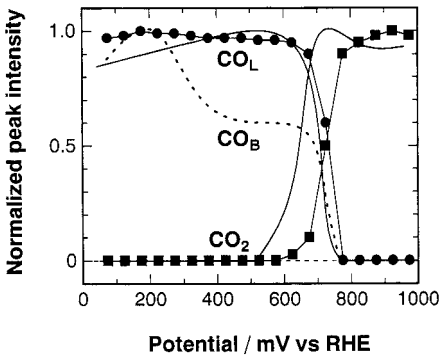

Figure 6. Potential dependencies of the normalized intensities of the linear and bridged CO or CO_2 absorption bands, on the $Pt_{27}Fe_{73}$ film electrode with the saturation coverage of CO ($\theta_{CO} = 0.55$) [(■) CO_2; (●) CO] and on the pure Pt electrode with approximately the same coverage of nonsaturated CO adlayer (line without data points).

the relationships between the normalized intensity of CO or CO_2 bands and the potential. On the Pt skin of the alloy electrode, the results (lines with date points) indicate the monotonic increase of CO_2 by the oxidation of the linear CO beyond ca. 0.6 V. Thus, it was confirmed that the linear potential dependence of the vibration frequency for the linear CO appears below the onset potential of the apparent CO oxidation, presumably resulting from the change of the electric field in the inner Helmholz layer, as discussed in the preceding section.

The relationships between the normalized intensity of the CO, CO_2 absorption bands at θ_{CO} = ca. 0.5 on the pure Pt electrode and the potential are shown in Figure 6 (lines without date points, cited from ref 26). Since IR spectra for the COOH, the presence of which was confirmed in our previous work,[26] were overlapping with those of CO_3^{2-} in some potential region, the similar quantitative potential dependence could not be shown in the figure. It is clear that after the internal transition of the bridged CO to linear CO below 0.4 V, each of them keeps a steady value until their oxidation commences in the more positive potential region. This result is well consistent with the dependence of the wavenumber for the stretching of the linear CO on the potential, shown in Figure 5 (line without data points).

It should be emphasized that both linear and bridged CO on the pure Pt begin to decrease and disappear almost at the same narrow potential region as that of the linear CO on the Pt skin of the alloy, i.e., 0.60−0.75 V, although the CO_2 production occurs at more than 0.1 V less-positive potential on the pure Pt. This clearly shows two important points: (1) the Pt skin surface on the alloy is not more active than that of the pure Pt for the direct oxidation both of linear and bridged CO, and (2) the lower onset potential for the oxidation of the CO adlayer on the pure Pt, found in the CV (see Figure 1B), is not due to the direct oxidation of the linear and/or bridged CO but due to the adsorbed COOH, induced by the surface reaction between the adsorbed CO and H_2O, as proposed in our previous work.[26] Then, the question arises how the excellent CO tolerance for the oxidation of H_2 containing CO impurity can be achieved on the Pt−Fe alloys as well as Pt−Ru, Pt−Co, Pt−Ni, or Pt−Mo.[10,11,13]

Recently, Ross and co-workers have worked extensively with the CO tolerance on Pt−Sn, Pt−Mo, and Pt−Ru alloys, but the CO content in H_2 is really high (>1%), far from that in the practical fuel cell condition.[3,41,42] Gottesfeld and co-workers also studied the mechanism on the Pt−Ru alloy in the practical fuel cell by means of mathematical simulation.[43] Both groups ascribed the CO tolerance to the formation of a few percent of CO free sites, which were thought to be prepared by the direct CO oxidation on the surface of exposing both alloy-component metals via the bifunctional mechanism originally proposed by Watanabe and Motoo.[1] But, as described above in the Introduction and Discussion, the active surfaces of the CO tolerant alloys as well as active alloys for O_2 reduction were covered with a few monolayers of Pt in our work, because of the dissolution of nonprecious metals from the alloy surfaces, except Pt−Ru alloys.[7−11,13] The Pt skins on the Pt alloys with different compositions had no particular high roughness or no exposure of particular crystalline facets in comparison with the pure Pt, but they exhibit the modified electronic structure, i.e., the increased d vacancy to the pure Pt, and the suppressed CO coverage less than ca. 0.5.[7−11,13] All of the SEIRAS data combined with the CVs in the present work well agree with the previous results, e.g., the high activity to H_2O oxidation, the disappearance of the multifold CO, or the weakened Pt−C bonding force, all of which must be brought by the increased d vacancy. However, no specifically high electrocatalytic activity for the direct CO oxidation was found, despite the high activity for the formation of OH species, which may be involved in the bifunctional CO oxidation mechanism. Despite the low catalytic activity for the direct CO oxidation, there remains the large number of CO free sites (mostly >50%) on the Pt skin surfaces having no alloying metals,[10,11,13] thus strongly indicating the CO tolerance mechanism to be different from that proposed in the previous works.[3,42,43] We therefore conclude the following mechanism for the CO tolerance on the Pt−Fe alloy: the lowered electron density of the 5d orbital of Pt decreases an electron back-donation from the Pt 5d orbital to the $2\pi^*$ orbital of CO and consequently suppresses CO−Pt bonding, resulting in the lowered CO coverage and the sufficient H_2 oxidation rate on the CO free sites. Although we have discussed the CO tolerant alloy based only on the data for $Pt_{27}Fe_{73}$ in this paper, we have obtained the similar results on the other Fe compositions and believe that the results on this representative alloy can be extended to all of the CO tolerant alloys. The detail discussion involving the other alloys will appear elsewhere.

Conclusion

The electronic property of the metal was modified when they were alloyed with another metal. In situ ATR-SEIRAS was used to investigate the oxidation process of adsorbed CO on the $Pt_{27}Fe_{73}$ alloy, the surface of which was covered with the Pt skin and had the increased d vacancy, as we reported previously. The linear CO with much lower saturated coverage was found on the skin of the alloy and had a higher mobility by the weakened Pt−C bonding than the pure Pt. An adsorbed HOOH species, which could not be observed at the pure Pt electrode, was clearly observed beyond 0.6 V in the electrolyte solution without CO. This formation could also be ascribed to the increased d vacancy in the Pt skin. Carbonate species were also detected around 1300−1450 cm^{-1}, which were possibly produced by the surface reaction of CO_2 with water or OH species. However, it was found that the Pt skin had no specifically high activity for the direct CO oxidation. Thus, we can conclude that the CO tolerance on the Pt−Fe alloy surface is brought about by the lowering of the CO coverage and the bonding strength to the Pt skin covering the alloy, but not via the facilitating oxidation.

Acknowledgment. This work was supported by the proposal-Based Advanced Industrial Technology R&D Program of the New Energy and Industrial Technology Development Organiza-

tion (NEDO) of Japan. This work was also partially supported by the Grants-in-Aid No. 09237104 for Scientific Research on Priority Area of "Electrochemistry of Ordered Interfaces" from the Ministry of Education, Science, Sports, and Culture, Japan. Useful comments by Professor Masatoshi Osawa (Hokkaido University) are greatly acknowledged. Y.-M.Z. acknowledges NEDO for the fellowship support.

References and Notes

(1) Watanabe, M.; Motoo, S. *J. Electroanl. Chem.* **1975**, *60*, 275.
(2) Beden, B.; Lamy, C.; De Tacconi, N. R.; Arvia, A. J. *Electrochim. Acta* **1990**, *35*, 691.
(3) Grgur, B. N.; Zhuang, G.; Markovic, N. M.; Ross, P. N. *J. Phys. Chem.* **1997**, *101*, 3910.
(4) Ianniello, R.; Schmidt, V. M.; Stimming, U.; Stumper, J.; Wallau, A. *Electrochim. Acta* **1994**, *39*, 1863.
(5) Kabbabi, A.; Faure, R.; Durand, R.; Beden, B.; Hahn, F.; Leger, J. M.; Lamy, C. *J. Electroanal. Chem.* **1998**, *444*, 41.
(6) Grgur, B. N.; Markovic, N. M.; Ross, P. N. *J. Phys. Chem.* **1998**, *102*, 2494.
(7) Toda, T.; Igarashi, H.; Watanabe, M. *J. Electroanal. Chem.* **1999**, *460*, 21.
(8) Toda, T.; Igarashi, H.; Watanabe, M. *J. Electrochem. Soc.* **1998**, *145*, 4185.
(9) Toda, T.; Igarashi, H.; Uchida, H.; Watanabe, M. *J. Electrochem. Soc.* **1999**, in press.
(10) Watanabe, M.; Igarashi, H.; Fujino, T. *Electrochemistry*, in press.
(11) Fujino, T. Thesis for M. Eng. Yamanashi University, 1996.
(12) Igarashi, H.; Fujino, T.; Watanabe, M. *J. Electroanal. Chem.* **1995**, *391*, 119.
(13) Watanabe, M.; Igarashi, H.; Fujino, T. *The 1997 Joint International Meeting of ECS and ISE*; Meeting Abstract 97-2; p 1238.
(14) Rodriguez, J. A.; Goodman, D. W. *Science* **1992**, *257*, 897.
(15) Wu, R.; Freeman, A. J. *Phys. Rev B* **1995**, *52*, 12419.
(16) Rodriguez, J. A.; Campbell, R. A.; Goodman, D. W. *J. Vac. Sci. Technol. A* **1991**, *9*, 1698.
(17) Atli, A.; Abon, M.; Beccat, P.; Bertolini, J. C.; Tardy, B. *Surf. Sci.* **1994**, *302*, 121.
(18) Ogletree, D. F.; Van Hove, M. A.; Somorjai, G. A. *Surf. Sci.* **1986**, *173*, 351.
(19) Lin, W.; Iwasita, T.; Vielstich, W. *J. Phys. Chem. B* **1999**, *103*, 3250.
(20) Morimoto, Y.; Yeager, E. B. *J. Electroanal. Chem.* **1998**, *441*, 77.
(21) Zou, S.; Villegas, I. Stuhlmann, C. Weaver, M. J. *Electrochim. Acta* **1998**, *43*, 2811.
(22) Ataka, K.; Yotsuyanagi, T.; Osawa, M. *J. Phys. Chem.* **1996**, *100*, 10664.
(23) Ataka, K.; Osawa, M. *Langmuir* **1998**, *14*, 951.
(24) Osawa, M. *Bull. Chem. Soc. Jpn.* **1997**, *70*, 2861.
(25) Sun, S.; Cai, W.; Wan, L.; Osawa, M. *J. Phys. Chem. B* **1999**, *103*, 2460.
(26) Zhu, Y.; Uchida, H.; Watanabe, M. *Langmuir* **1999**, *15*, 8757.
(27) Watanabe, M.; Motoo, S. *J. Electroanal. Chem.* **1986**, *206*, 197.
(28) Norton, P. R.; Richards, P. J. *Surf. Sci.* **1975**, *49*, 567.
(29) Shaw, K.; Christensen, P.; Hamnett, A. *Electrochim. Acta* **1996**, *41*, 719.
(30) Brooker, J.; Christensen, P. A.; Hamnett, A.; He, R.; Paliteiro, C. A. *Faraday Discuss.* **1992**, *94*, 339.
(31) Adzic, R. *Mod. Aspects Electrochem.* **1990**, *21*, 163.
(32) Leung, L.-W. H.; Chang, S.-C.; Weaver, M. J. *J. Chem. Phys.* **1989**, *90*, 7426.
(33) Lambert, D. K. *J. Chem. Phys.* **1988**, *89*, 3847.
(34) Oliver, B. G.; Davis, A. R. *Can. J. Chem.* **1973**, *51*, 698.
(35) Iwasita, T.; Rodes, A.; Pastor, E. *J. Electroanal. Chem.* **1995**, *383*, 181.
(36) Markovits, A.; Garcia-Hernandez, M.; Ricart, J. M.; Illas, F. *J. Phys. Chem. B* **1999**, *103*, 509.
(37) Fujita, J.; Martell, A. E.; Nakamoto, K. *J. Chem. Phys.* **1962**, *36*, 339.
(38) Lambert, D. K. *J. Chem. Phys.* **1988**, *89*, 3847.
(39) Anderson, B. *J. Electroanal. Chem.* **1990**, *280*, 37.
(40) Lucas, A. A.; Mahan, G. D. In *Vibratios in Adsorbed Layers, Conference Records Series of KFA*; Ibach, H., Lehwald, S., Eds.; KFA: Julich, 1978.
(41) Gasteiger, H. A.; Markovic, N.; Ross, P. N. Jr, Cairns, E. J. *J. Phys. Chem.* **1994**, *98*, 617
(42) Gasteiger, H.; Mrkovic, N.; Ross, P. *J. Phys. Chem.* **1995**, *99*, 8945.
(43) Zawodzinski, T. A.; Springer, T. E.; Gottesfeld, S. *The 1997 Joint International Meeting of ECS and ISE*; Meeting Abstact 97-2; p 1228.